J Mater Sci (2006) 41:7483–7491
DOI 10.1007/s10853-006-0724-1

Studies on photoconductivity, photovoltaic effect and photoluminescence in chemically deposited $(Cd_{0.95}–Pb_{0.05})S:CdCl_2$,Dy/Y films

S. Bhushan · Swati Shrivastava · Ashok Shrivastava

Received: 30 August 2005 / Accepted: 5 December 2005 / Published online: 20 September 2006

Abstract Results of photoconductivity (PC) and photoluminescence (PL) are presented for films of $(Cd_{0.95}–Pb_{0.05})S:CdCl_2$,Dy/Y prepared at 60 °C and RT on glass substrates. PC is found to be enhanced in films prepared at 60 °C particularly in presence of impurities. PL is found to be stronger in films prepared at RT. While films prepared in presence of Dy show one peak in green yellow region, those prepared in presence of Y show two peaks one in blue and other in green yellow regions. Results of SEM, XRD, and optical absorption spectra, which have been used to characterize the materials, are presented. Photovoltaic efficiency in $(Cd_{0.95}–Pb_{0.05})S:CdCl_2$,Dy films has been found to be ~5%.

Introduction

CdS and PbS both are important materials for photoconductivity (PC) applications like xerography and IR detection, etc. and have drawn interest of a number of research workers, particularly using chemical deposition technique. While a number of workers [1–4] prepared PbS films on different substrates like semiconducting materials and ferroelectric ceramics/dielectrics, CdS films were also attempted by a large number of workers [5–9]. Particularly in CdS many fold improvements in electro-optical properties were reported by Nair et al. [1] and Bhushan et al. [10–12]. Such investigations inspired us to work on (Cd–Pb)S films. PC of (Cd–Pb)S films using NaF/$CdCl_2$ as flux and La, Nd, and Sm as impurities were recently reported by Bhushan and co-workers [13–17]. It was found that in presence of $CdCl_2$ the PC gains were higher as compared to those in presence of NaF. It was also found [17] that in photoluminescence (PL) of Sm doped (Cd–Pb)S films prepared in a water bath at 60 °C an emission peak appeared in the green–yellow region under the excitation of 365 nm Hg. Photovoltaic effects were also reported recently [18] in films of (Cd–Pb)S and (Cd–Zn)S using La and Pr as impurities with an efficiency ~3.12–3.71%. In the present work results of PC and photovoltaic (PV) studies and PL are presented on films of (Cd–Pb)S films using $CdCl_2$ as flux and new impurities as Dy and Y. These films were prepared by dipping technique either at room temperature (RT) or at 60 °C in a water bath. It has been found that quite intense PL occurs in films prepared at RT and PC becomes prominent in films prepared at 60 °C. Improved PV has also been found. For characterization results of PC excitation and optical absorption spectra, XRD and SEM studies are also presented in the present paper.

Experimental

Film preparation

The films were prepared on substrates of microscopic glass slides/conducting glass plates. Conducting glass plates were used in films of photovoltaic studies only. These plates were prepared by depositing conducting layer of SnO_2 using a glass sprayer fabricated at this

---

S. Bhushan (✉) · S. Shrivastava · A. Shrivastava
School of Studies in Physics, Pt. Ravishankar Shukla
University, Raipur (C.G.) 492010, India
e-mail: bhushan_s31@rediffmail.com

place. The resistivity of these plates was ~20 Ω/cm^2. The substrates were cleaned using HCl, acetone, distilled water, and ultrasonic cleaner before depositing the films. The cleaned substrates were dipped into a mixture of solutions of 1 M cadmium acetate, lead acetate, thiourea along with triethanolamine and aqueous ammonia (all analytical reagent) at either RT or at 60 °C in a water bath. The proportions of aqueous ammonia were also varied in some cases. Doped films were prepared by adding to the original mixture 0.01 M solutions of $CdCl_2$ and Y_2O_3. Since Y_2O_3 being insoluble in distilled water, its solution was prepared in conc. H_2SO_4. All other solutions were prepared in double distilled water. The pH value of such mixture was found to vary in the range 9.5–11. The deposition of the films was based on precipitation followed by condensation. In the beginning when precipitation started stirring was done after that the deposition was made in the static condition. After deposition the films were cleaned with distilled water and then dried by keeping them in open atmosphere at RT. Annealing of the films was done at 350 °C for 3 min. The thickness of the films were measured by mass difference method using a microbalance and were found as 0.2545 μm [60 °C deposition (for 1 h)] and 1.56-2.04 μm [RT depositions (for 16 h, 18 h, and 20 h)] for different films.

Cells

For PC studies co-planar electrodes (1.5 mm wide and 24 mm long at a separation of 2 mm) were formed by applying colloidal silver paint to the surface of the films. The photocurrents were measured by exposing central area, i.e., by removing the uncovered area beyond the electrodes. For PV measurements sliver electrode in 1 cm^2 area was painted on the back surface of the films. For photoluminescence studies the deposited films were exposed directly to the exciting radiation.

Measuring instruments

The PC rise and decay studies were made by exciting with incandescent bulb of 100 W (power 8 mW) and noting the photocurrent as a function of time by a Nanometer (DNM 121). For PC excitation spectral studies different wavelengths were selected by passing the radiation from an incandescent bulb of 1 kW through a prism monochromator and noting the photocurrent corresponding to different exciting wavelengths thus obtained. PV studies were made by using a bulb of 100 W (power 6 mW). The current and voltage were measured by using the earlier mentioned nanometer and a digital multi-meter (scientific HM 5011-3), respectively. Optical absorption studies were made by using a Varian (UV–vis)DMS-100 spectrophotometer. PL studies were performed by exciting the cell with 365 nm Hg radiation obtained by using a high pressure Hg lamp and a Carl–Zeiss Interference filter. For recording the PL intensity RCA 6217 photomultiplier tube, which was operated by a highly regulated power supply, was used. The corresponding current was recorded by a polyflex galvanometer (10^{-9} A/mm). Emission spectra were studied by using a Thermo Jarrel Ash monochromator. SEM and XRD studies were performed at University of Delhi using a computerized Shimadzu diffractometer [model—98 XRD; λ = 1.54056 Å (CuKα_1)].

Results and discussion

SEM studies

The SEM micrographs of (Cd–Pb)S:$CdCl_2$,Dy and (Cd–Pb)S:$CdCl_2$,Y prepared at 60 °C and RT are presented in Figs. 1a, b and 2a, b, respectively. In all the cases almost spherical shaped grains are observed in different cases. In both the cases some bigger grains are also observed.

XRD studies

The XRD diffractogram of (Cd–Pb)S :$CdCl_2$,Y (as an example) is shown in Fig. 3. The assignments of peaks were made by comparing with the ASTM data and through evaluation of lattice constants. The different assigned peaks are mentioned in the figure and the corresponding data are summarized in Table 1. It is noted that prominent lines of CdS and PbS are observed. The average particle size (D) was estimated from the full width at half-maximum (FWHM) of the diffraction peaks, using Sherrer's formula [19]:

$$D = K\lambda/\beta_{1/2}\cos\theta \quad (1)$$

where λ is the wavelength of X-ray, θ the Bragg's angle (in radian), K a constant, which depends on the grain shape, and $\beta_{1/2}$ is the full width at half-maximum. The average particle size is found to be of the order of 3.347 Å.

PC studies

The nature of rise and decay of photocurrents have been found to be similar to those of

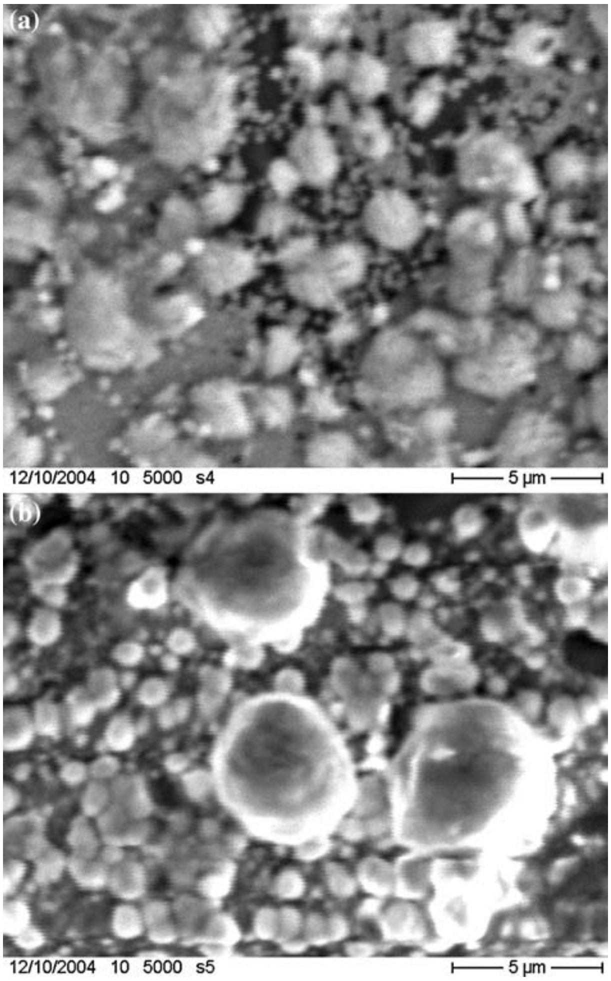

Fig. 1 SEM micrograph of (**a**) $(Cd_{0.95}–Pb_{0.05})S:CdCl_2,Dy$ prepared at 60 °C; (**b**) $(Cd_{0.95}–Pb_{0.05})S:CdCl_2,Dy$ prepared at RT

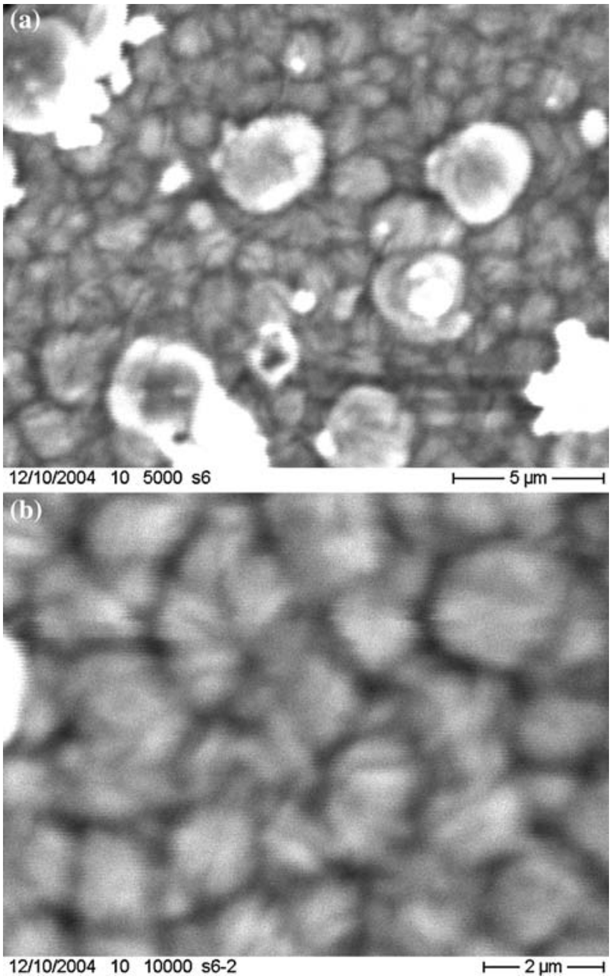

Fig. 2 SEM micrograph of (**a**) $(Cd_{0.95}–Pb_{0.05})S:CdCl_2,Y$ prepared at 60 °C; (**b**) $(Cd_{0.95}–Pb_{0.05})S:CdCl_2,Y$ prepared at RT

$(Cd_{0.95}–Pb_{0.05})S:CdCl_2,Sm$ as reported earlier [17]. However, the values of the ratio of saturated photocurrent (I_{pc}) to dark current (I_{dc}) were found to be different in certain cases. In CdS this ratio was found to be: 1.594×10^5 (unannealed); 4.15×10^5 (annealed) which improved to 1.925×10^6 (unannealed); 1.691×10^7 (annealed) in $(Cd_{0.95}–Pb_{0.05})S$. These values enhanced to 0.477×10^7 (unannealed); 2.071×10^7 (annealed) in $(Cd_{0.95}–Pb_{0.05})S:CdCl_2$ (4 ml). These values were further enhanced in presence of impurities as follows: $(Cd_{0.95}–Pb_{0.05})S:CdCl_2$ (4 ml),Dy_2O_3 (2 ml) = 1.06×10^7 (unannealed); 3.404×10^7 (annealed); $(Cd_{0.95}–Pb_{0.05})S:CdCl_2$ (4 ml),Y_2O_3 (4 ml) = 0.976×10^7 (unannealed); 2.3×10^7 (annealed). It should be noted that all these values concern to the films prepared at 60 °C. On analyzing the decay curves it was found that two kinds of traps were effective in all the systems with values ranging between 0.746 and 0.846 eV. Similarly the values of life time and mobility were also obtained from the analysis of rise and decay curves. It was found that the values of life time and mobility also varied for the different films as follows: life time 13.28–212.8 s; mobility: 32–373.34 cm^2/V s. The RT preparation

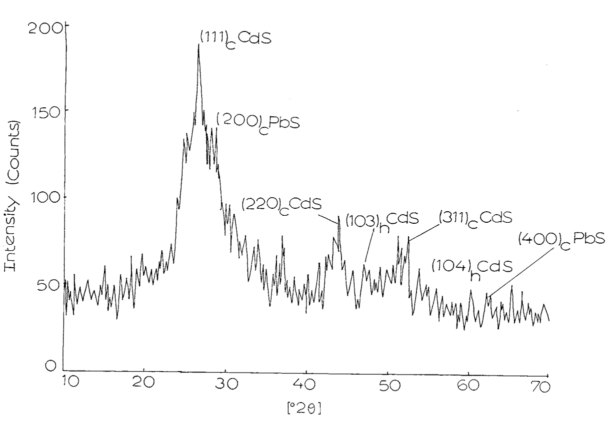

Fig. 3 X-ray diffractogram of $(Cd_{0.95}–Pb_{0.05})S:CdCl_2,Y$

Table 1 XRD data of $(Cd_{0.95}–Pb_{0.05})S:CdCl_2,Y$ film

S.No.	*d*-values (Å)		Relative intensities		*hkl*	Lattice constant (Å)	
	Observed	Reported	Observed	Reported		Observed	Reported
1	3.3746	3.36	94.5	100	(111)c-CdS	$a = 5.84$	$a = 5.833$
2	3.1198	2.969	68.75	100	(200)c-PbS	$a = 6.23$	$a = 5.936$
3	2.0638	2.058	44	80	(220)c-CdS	$a = 5.83$	$a = 5.833$
4	1.9294	1.898	31	42	(103)h-CdS	$c/a = 1.66$	$c/a = 1.633$
5	1.7417	1.761	37.5	90	(311)c-CdS	$a = 5.77$	$a = 5.833$
6	1.5336	1.048	25.5	2	(104)h-CdS	$c/a = 1.64$	$c/a = 1.633$
7	1.4894	1.048	24.5	10	(400)c-PbS	$a = 5.95$	$a = 5.936$

needed higher times of preparation. The films were prepared at 16 h, 18 h, and 20 h deposition and the highest value of I_{pc}/I_{dc} was observed as 2.175×10^4 in the third case. The percentage of ammonia was also varied from 30% to 80% and it was found that the ratio of I_{pc}/I_{dc} decreased correspondingly. The values for 80% ammonia, for example, are as follows $(Cd_{0.95}–Pb_{0.05})S:CdCl_2,Dy$: $I_{pc}/I_{dc} = 8$; $(Cd_{0.95}–Pb_{0.05})S:CdCl_2,Y$: $I_{pc}/I_{dc} = 25$. The trap depth values of these samples were almost similar (varied between 0.729 eV and 0.767 eV) however the values of life time and mobility were found to be quite different. Life time varied between 0.056 s and 6.32 s and mobility was found to be in the range 1.33–9.17 cm^2/V s.

PC excitation and optical absorption spectral studies

The PC excitation spectra of different (Cd–Pb)S films are shown in Fig. 4 for unannealed condition. A strong peak corresponding to the bandgap excitation is observed in all the cases. Enhancement in photocurrent is observed in presence of $CdCl_2$,Dy and Y. Due to annealing increase in photocurrent and change in peak positions are also observed. In some of the curves shoulders are also seen which occur due to presence of impurities added. The bandgaps obtained from peak positions are summarized in Table 2. The corresponding wavelengths are also mentioned in the table. It is also observed that as expected the bandgaps decrease due to increase in concentration of Pb.

The optical absorption spectra of different (Cd–Pb)S films are shown in Fig. 5 for unannealed condition. Due to annealing a similar nature was found except for some changes due to which the bandgaps differ to some extent. From the Tauc's plots $(\alpha h\nu^2$ versus $h\nu)$ the bandgaps were determined and the corresponding values are listed in Table 3. The values of bandgaps obtained from two kinds of studies, i.e., the PC excitation spectra and optical absorption spectra are seen to be almost similar, although there is little increase in bandgaps due to annealing.

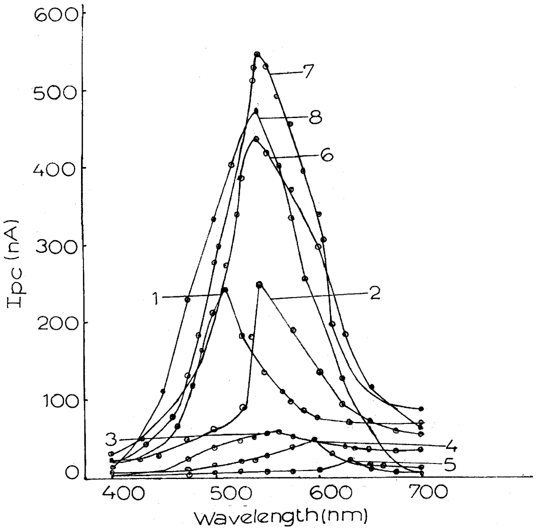

Fig. 4 Photoconductivity excitation spectra of different (Cd–Pb)S:$CdCl_2$,Dy/Y unannealed films. 1. CdS; 2. $(Cd_{0.95}–Pb_{0.05})S$; 3. $(Cd_{0.90}–Pb_{0.10})S$; 4. $(Cd_{0.85}–Pb_{0.15})S$; 5. $(Cd_{0.80}–Pb_{0.20})S$; 6. $(Cd_{0.95}–Pb_{0.05})S:CdCl_2$ (4 ml); 7. $(Cd_{0.95}–Pb_{0.05})S:CdCl_2$ (4 ml),Dy (2 ml); 8. $(Cd_{0.95}–Pb_{0.05})S:CdCl_2$ (4 ml),Y (4 ml)

PV effect

The PV measurements were made for samples in presence of Dy. As mentioned earlier conducting glass plate served the purpose of one electrode and colloidal silver paste as the other electrode. Thus, it can behave as M–S contact. The corresponding *I–V* curves for (Cd–Pb)S:$CdCl_2$,Dy system are shown in Fig. 6. The values of short circuit current (I_{sc}), open circuit voltage (V_{oc}), fill factor ($I_m \times V_m/I_{sc} \times V_{oc}$ where I_m and V_m are the values corresponding to maximum power rectangle) and the efficiency ($\eta = I_m \times V_m/P_{in}$ where P_{in} is input power: $P = 6$ mW) are summarized in Table 4. A maximum value of efficiency 5.49% is obtained. In view of the simplicity of the method such a

Table 2 Bandgaps obtained from photoconductivity excitation spectral studies of different (Cd–Pb)S films

S. No.	System	Unannealed film		Annealed film	
		Peak wavelength (nm)	Bandgap (eV)	Peak wavelength (nm)	Bandgap (eV)
1	CdS	510	2.44	510	2.44
2	$(Cd_{0.95}–Pb_{0.05})S$	540	2.30	537	2.31
3	$(Cd_{0.90}–Pb_{0.10})S$	560	2.22	552	2.25
4	$(Cd_{0.85}–Pb_{0.15})S$	591	2.10	590	2.11
5	$(Cd_{0.80}–Pb_{0.20})S$	630	1.97	627	1.98
6	$(Cd_{0.95}–Pb_{0.05})S:CdCl_2$ (4 ml)	540	2.30	537	2.31
7	$(Cd_{0.95}–Pb_{0.05})S:CdCl_2$ (4 ml), Dy (2 ml)	540	2.30	537	2.31
8	$(Cd_{0.95}–Pb_{0.05})S:CdCl_2$ (4 ml), Y (4 ml)	540	2.30	537	2.31

Temperature of deposition: 60 °C; time of deposition: 1 h; annealing temperature: 350 °C; time of annealing: 3 min

value of efficiency should not be considered as very low. It is also observed that due to presence of impurities the ratio I_{pc}/I_{dc} increases where as the efficiency of PV effect decreases. This is quite obvious because while PC is a majority carrier phenomenon, the PV effect is a minority carrier one.

PL spectral studies

The PL emission spectra of CdS, $(Cd_{0.95}–Pb_{0.05})S$, and $(Cd_{0.95}–Pb_{0.05})S:CdCl_2$ films prepared at 60 °C and RT consisted of peaks as follows: CdS: 533.2 nm (60 °C; Int. 121) and 545.2 nm (RT; Int. 193); $(Cd_{0.95}–Pb_{0.05})S$: 530 nm (60 °C ; Int. 130) and 526.4 nm (RT; Int. 149); $(Cd_{0.95}–Pb_{0.05})S:CdCl_2$ (4 ml): 531 nm (60 °C; Int. 139) and 532.3 nm (RT; Int. 151). Thus, the intensity in presence of $CdCl_2$ is improved and peak positions shift to higher wavelength side as compared to that of $(Cd_{0.95}–Pb_{0.05})S$. The PL emission spectra of different $(Cd_{0.95}–Pb_{0.05})S:CdCl_2$,Dy was investigated at varied concentration of Dy_2O_3, i.e., at 2 ml, 4 ml, 6 ml, 8 ml, and 10 ml. It was found that the best emission occurred at 8 ml of Dy_2O_3. Corresponding results of the films prepared at 60 °C and RT are shown in Fig. 7. RT preparation needed higher times of deposition. Emission was checked at three times of preparation 16 h, 18 h, and 20 h. These spectra are also included in Fig. 7. It is observed that higher emission occurs for 16 h deposition time. Depositions at lower times than 16 h did not yield good films. With this time of deposition the concentration of ammonia was varied. It is found that higher emission occurs at higher concentrations of ammonia. Such results are shown in Fig. 8. The peak positions and intensities under different conditions are summarized in Table 5. The PL emission spectra of $(Cd_{0.95}–Pb_{0.05})S:CdCl_2$,Y was found to consist of two peaks with a maximum volume of Y_2O_3 as 8 ml. Results of this sample prepared at RT and 60 °C are shown in Figs. 9 and 10, respectively. Results varying concentrations of ammonia in this system are shown in Fig. 11. The corresponding peak positions and intensities are also summarized in Table 5. It is observed that the films prepared at RT showed better emission compared to those prepared at 60 °C in water bath.

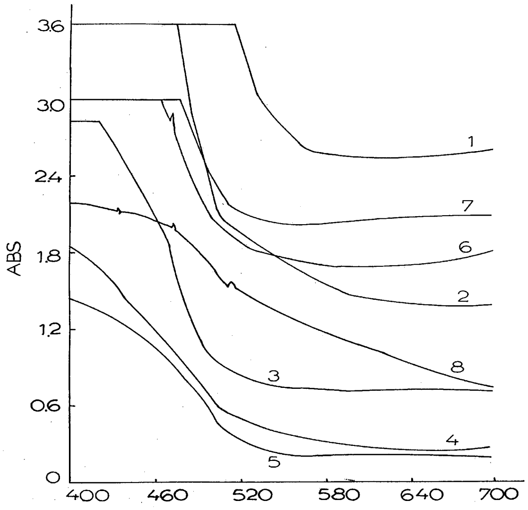

Fig. 5 Optical absorption spectra of different (Cd–Pb)S: $CdCl_2$,Dy/Y unannealed films. 1. CdS; 2. $(Cd_{0.95}–Pb_{0.05})S$; 3. $(Cd_{0.90}–Pb_{0.10})S$; 4. $(Cd_{0.85}–Pb_{0.15})S$; 5. $(Cd_{0.80}—Pb_{0.20})S$; 6. $(Cd_{0.95}–Pb_{0.05})S:CdCl_2$ (4 ml); 7. $(Cd_{0.95}–Pb_{0.05})S:CdCl_2$ (4 ml),Dy (2 ml); 8. $(Cd_{0.95}–Pb_{0.05})S:CdCl_2$ (4 ml),Y (4 ml)

Normally stoichiometric differences are expected in such kinds of preparation. Therefore, the emission peak of CdS observed at 533.2 nm may be associated with the acceptor levels formed by Cd vacancies [16]. However, in (Cd–Pb)S the bandgap decreases and hence the emission energy is shifted on higher wavelength side. Due to inclusion of impurities (Dy) the emission peaks again shift towards mostly on higher wavelength side showing the substitution of impurities

Table 3 Bandgaps obtained from optical absorption spectral studies of different (Cd–Pb)S films

S. No.	System	Bandgap (eV)	
		Unannealed	Annealed
1	CdS	2.42	2.44
2	$(Cd_{0.95}–Pb_{0.05})S$	2.24	2.33
3	$(Cd_{0.90}–Pb_{0.10})S$	2.21	2.26
4	$(Cd_{0.85}–Pb_{0.15})S$	2.08	2.14
5	$(Cd_{0.80}–Pb_{0.20})S$	1.95	2.01
6	$(Cd_{0.95}–Pb_{0.05})S:CdCl_2$ (4 ml)	2.24	2.33
7	$(Cd_{0.95}–Pb_{0.05})S:CdCl_2$,Dy (2 ml)	2.24	2.33
8	$(Cd_{0.95}–Pb_{0.05})S:CdCl_2$,Y (4 ml)	2.24	2.33

Temperature of deposition: 60 °C; time of deposition: 1 h; annealing temperature: 350 °C; time of annealing: 3 min

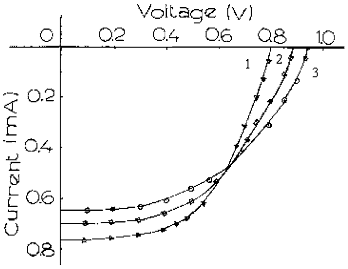

Fig. 6 *I–V* characteristics of different $(Cd_{0.95}–Pb_{0.05})S:CdCl_2$,Dy films. 1. (Cd-Pb)S (–Δ–); 2. (Cd–Pb)S:$CdCl_2$ (–□–); 3. (Cd–Pb)S:$CdCl_2$,Dy (–O–)

in the lattice. Since deposition of such films is favored in alkaline medium at higher concentrations of ammonia, i.e., at higher pH values better conditions of growth is expected. Thus, higher emissions are observed at higher concentrations of ammonia. Since the observed emission shows a broader peak, therefore, emission cannot be related to direct transition in rare-earth elements. It may be related to a transitions corresponding to defect levels and rare earth levels. In an earlier work on ZnS doped with Dy alone two peaks were reported by Rothschild [20]; one broad peak at 4,680 Å and a narrow emission at 5,800 Å related to $^4F_{9/2} \rightarrow {}^6H_{15/2}$ and $^4F_{9/2} \rightarrow {}^6H_{13/2}$ transition of Dy^{+++}, respectively. Anderson et al. [21] reported some more emission due to Dy in ZnS: 4,800 Å ($^4F_{9/2} \rightarrow {}^6H_{15/2}$); 5,740 Å ($^4F_{9/2} \rightarrow {}^6H_{13/2}$); 6,600 Å ($^4F_{9/2} \rightarrow {}^6H_{11/2}$); 7,460 Å ($^4F_{9/2} \rightarrow {}^6H_{9/2}$); 8,400 Å ($^4F_{9/2} \rightarrow {}^6H_{7/2}$). This clearly indicates that emission in our case does not belong to direct transition in energy level of Dy. However, since there is shift in emission due to Dy, therefore, the observed emission is related to a combination of defect and rare earth levels.

Further, due to incorporation of Y two bands are observed in blue and green yellow regions with maximum intensities for 8 ml of Y_2O_3. Both of these show shift towards higher wavelength side with increase in concentration of Y. Thus, both of this may correspond to transition in the energy level of Y. Kröger and Dikhoff [22] found that incorporation of monovalent cations in a lattice of ZnS (divalent ions) was possible when lead of positive charge resulting from the substitution of a monovalent cation for a divalent one was compensated. This compensation was made by trivalent cation like Y. Thus it may also be possible that the band in the green yellow region may appear due to combination of defect and levels of Y. It should be noted that the undoped material already shows emission given in the green region. However, the blue band seems to appear due to transition in Y.

The emission intensities for the films prepared at RT are higher. Films prepared at 60 °C show lower emission, which may result due to involvement of some quenching centers. It should be noted that annealed films showed high photocurrent as compared to unannealed films but in PL study unannealed films showed higher intensity whereas annealed films do not show PL emission.

Table 4 Results of photovoltaic studies

S. No.	System	I_{sc} (mA)	V_{oc} (V)	I_m (mA)	V_m (V)	Fill factor	Efficiency (%)
1	$(Cd_{0.95}–Pb_{0.05})S$	0.76	0.80	0.60	0.55	0.542	5.49
2	$(Cd_{0.95}–Pb_{0.05})S:CdCl_2$ (4 ml)	0.70	0.88	0.56	0.55	0.50	5.13
3	$(Cd_{0.95}–Pb_{0.05})S$: $CdCl_2$ 4 ml),Dy(2 ml)	0.65	0.95	0.47	0.64	0.487	5.01

Temperature of deposition: 60 °C, Time of deposition: 1 h

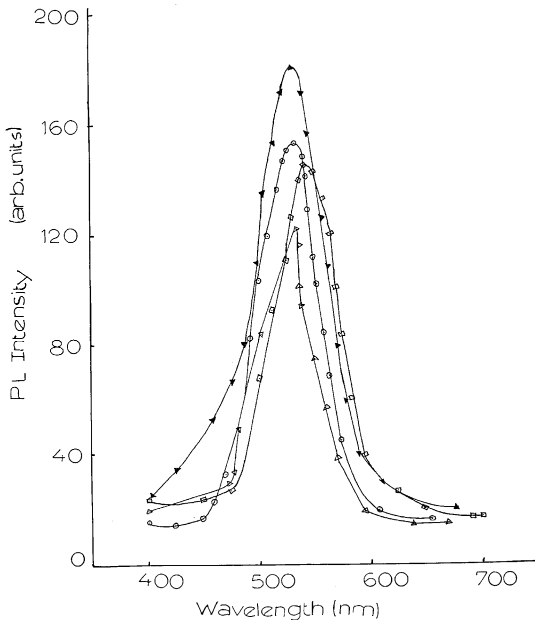

Fig. 7 PL emission spectra of $(Cd_{0.95}–Pb_{0.05})S:CdCl_2,Dy$ (8 ml) prepared under different conditions: (–□–) 60 °C; (–▲–) RT 16 h; (–O–) RT 18 h; (–Δ–) 20 h

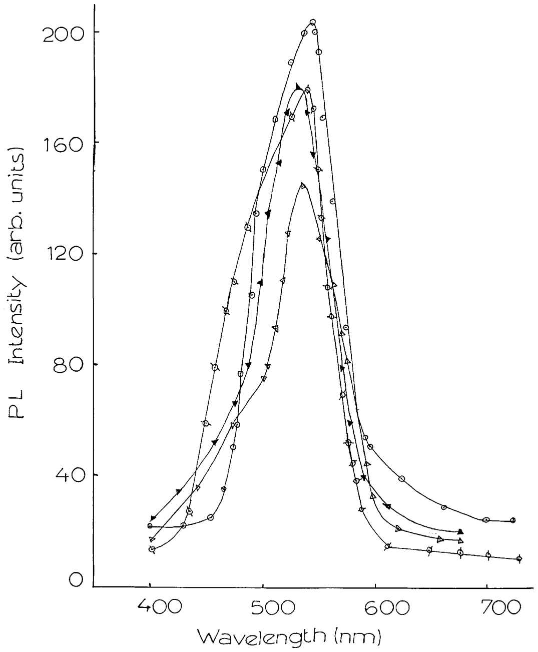

Fig. 8 PL emission spectra of $(Cd_{0.95}–Pb_{0.05})S:CdCl_2,Dy$ films prepared at RT using different concentrations of ammonia: (–O–) 30%; (–Δ–) 40%; (–Φ–) 60%; (–▲–) 80%

Table 5 Photoluminescence emission spectra studies of different $(Cd–Pb)S:CdCl_2,Dy/Y$ films

S.No.	System	Films prepared at 60°C Peak position (nm)	(Intensity)	Films prepared at RT Peak position (nm)	(Intensity)	
1.	$(Cd_{0.95}$-$Pb_{0.05})S:CdCl_2$ (4ml),Dy(8ml)	541.2	(145)	532.2	(182)	30% Ammonia, 16 hrs. deposition
				533.2	(154)	-----do------ 18 hrs. deposition
				534.4	(122)	-----do------ 20 hrs. deposition
				535.2	(146)	40%Ammonia,16 hrs.deposition
				537.4	(180)	60%Ammonia,16 hrs. deposition
				540	(205)	80%Ammonia,16 hrs.deposition
2.	$(Cd_{0.95}$-$Pb_{0.05})S:CdCl_2$ (4ml),Y(8ml)	545.2	(140)	554.2	(153)	30% Ammonia 16 hrs. deposition
		480	(90)	486	(119)	
				507.4	(156)	40%Ammonia, 16 hrs.deposition
				486.6	(117)	
				534.6	(177)	60%Ammonia, 16 hrs. deposition
				462.4	(60)	
				561.2	(205)	80%Ammonia, 16 hrs.deposition
				487.2	(141)	

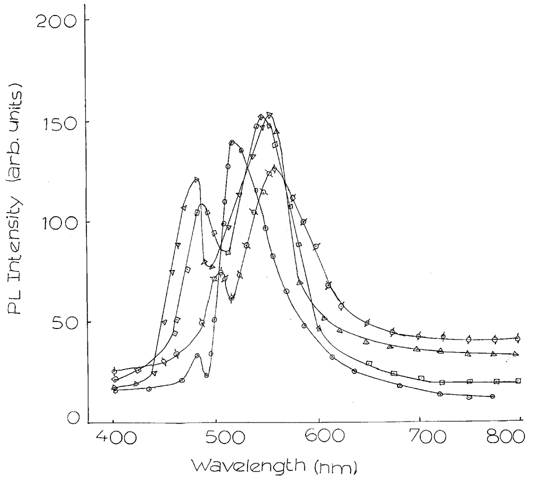

Fig. 9 PL emission spectra of $(Cd_{0.95}–Pb_{0.05})S:CdCl_2,Y$ films prepared at RT using different volumes of Y_2O_3: (–□–) 4 ml; (–Δ–) 6 ml; (–Φ–) 8 ml; (–O–) 10 ml

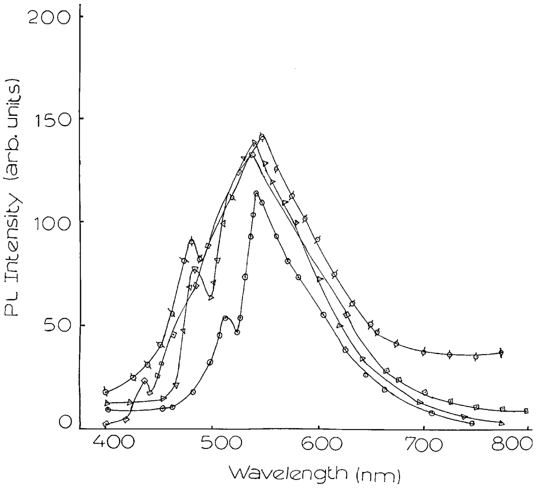

Fig. 10 PL emission spectra of $(Cd_{0.95}–Pb_{0.05})S:CdCl_2,Y$ films prepared at 60 °C using different volumes of Y_2O_3: (–□–) 4 ml; (–Δ–) 6 ml; (–Φ–) 8 ml; (–O–) 10 ml

Conclusion

In the films of $(Cd–Pb)S:CdCl_2,Dy/Y$ prepared at RT and 60 °C in a water bath, both PC and PL are observed. The PC is found to be quite strong ($I_{pc}/I_{dc} \sim 10^7$) in films of latter type whereas PL is found to be strong in intensities in the films of former type. While incorporation of Dy results in one strong peak in PL emission spectra, two peaks are found in presence of Y. Results of optical absorption support formation of a common lattice of (Cd–Pb)S which has lower bandgap of direct nature than that of CdS. In some of the films PV efficiency of the order of 5% has also been observed. Results of XRD studies show the particle sizes in nano range. SEM studies show spherical type grains.

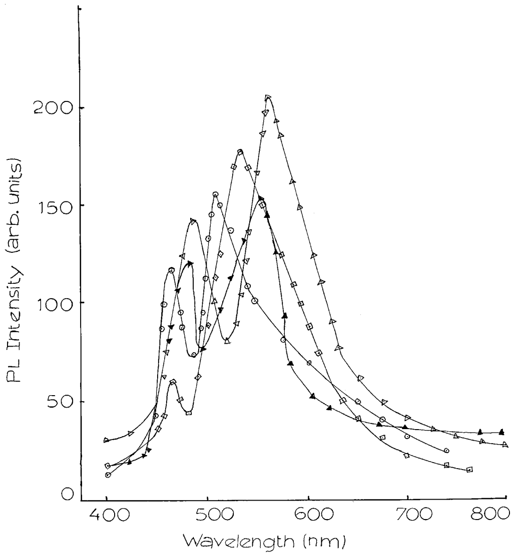

Fig. 11 PL emission spectra of $(Cd_{0.95}–Pb_{0.05})S:CdCl_2,Y$ films prepared at RT using different concentrations of ammonia : (–▲–) 30%; (–O–) 40%; (–□–) 60% ; (–Δ–) 80%

Acknowledgements Thanks are due to Dr. P.D. Sahare of Delhi University for SEM and XRD studies. Authors are also grateful to CCOST for sponsoring this work by granting a research project along with a fellowship to one of them (S.S.).

References

1. Nair PK, Nair MTS, Fernandez A, Ocampa M (1989) J Phys D Appl Phys 22:829
2. Tamashyunas R, Pytrauskas M, Vaitkus Yu, Sinyus Ya, Graska R, Vlaskin A (1991) Sov Phys Semicond (USA), 25:623, Translation of Fiz Tekh Poluprovodn (USSR) 25:1070
3. Pentia E, Pentilie L, Tivarus C, Pintilie C, Botila T (2001) Mater Sci Eng 23:80
4. Gudaev OA, Malinovaski (1991) Thin Solid Films 35:198
5. Isshiki M, Endo T, Masumot K (1990) J Electrochem Soc 137:2697
6. Pintilie L, Pentia E, Pintilie I, Petre D (1997) Mater Sci Eng B (Solid State Mater Adv Technol) 44:403
7. Pintilie L, Pentia E, Pintilie I, BotilaT, Constantin C (2000) Appl Phys Lett 76:1890
8. Karanjai MK, Dasgupta D (1987) Thin Solid Films 155:309
9. Nair MTS, Nair PK (1987) Solar Energy Mater Sol Cells 15:441
10. Bhushan S, Sharma SK (1990) J Phys D Appl Phys 23:909
11. Bhushan S, Thakur D (1992) J Mater Sci (Mater Electron) 3:35
12. Shrivastava S, Bhushan S (1996) Ind J Pure Appl Phys 34:106
13. Bhushan S, Mukherjee M, Bose P (2001) Radiat Eff Defect Solid 153:367
14. Mukherjee M, Bose P, Bhushan S (2001) Ind J Pure Appl Phys 39:804

15. Bhushan S, Mukherjee M, Bose P (2002) J Mater Sci (Mater Electron) 13:581
16. Mukherjee M, Bhushan S (2003) Opt Mater 22:51
17. Mukherjee M, Bhushan S (2003) Radiat Eff Defect Solid 158:491
18. Chandra T, Bhushan S (2004) J Mater Sci 39:6303
19. Klug H, Alexander L (1962) X-ray diffraction procedures, John Willey & Sons Inc., New York, p. 491
20. Rothschild S (1958) Proc Int Conf Sol State Phys Electr Telecomm 4(Pt 2):705
21. Anderson WW, Razi S, Walsh DJ (1965) J Chem Phys 43:1153
22. Kröger FA, Dikhoff J (1950) Physica 16:297